ELSEVIER

Journal of Photochemistry and Photobiology
A: Chemistry 86 (1995) 191–196

Journal of PHOTOCHEMISTRY AND PHOTOBIOLOGY A: CHEMISTRY

Photoreduction of carbon dioxide using chalcogenide semiconductor microcrystals

Hiroshi Inoue, Hiroshi Moriwaki, Kotaro Maeda, Hiroshi Yoneyama *

Department of Applied Chemistry, Faculty of Engineering, Osaka University, Yamada-oka 2-1, Suita, Osaka 565, Japan

Received 31 January 1994; accepted 19 July 1994

Abstract

The photoreduction behaviour of CO_2 on cadmium-loaded ZnS microcrystals and ZnS–CdS solid solution microcrystals was investigated. The photoreduction product on Cd-loaded ZnS was formate, and the highest quantum efficiency of production was 32.5%, which was twice as large as that obtained on bare ZnS microcrystals. However, solid solutions of ZnS–CdS microcrystals did not exhibit high activities for the photoreduction of CO_2. With increasing mole fraction of CdS, the activities for formate production decreased, and the production of CO was observed for a CdS mole fraction of 0.5–0.67.

Keywords: Photoreduction; Chalcogenide semiconductor

1. Introduction

The light-induced reduction of CO_2 molecules in aqueous solutions using semiconductor photocatalysts has been investigated extensively [1–15]. Two-electron reduction products, such as carbon monoxide and formate, and four- and six-electron reduction products, such as formaldehyde and methanol, have been reported. However, the quantum efficiencies of these reductions are very low, except for the use of ZnS microcrystals in the presence of highly reactive hole scavengers [3,13,14].

In a previous report, using ZnS microcrystals as photocatalyst, 2-propanol was used as hole scavenger. The significance of the use of this hole scavenger is that the light energy can be stored in the light-induced reaction given by

$$CO_2 + (CH_3)_2CHOH \longrightarrow HCOOH + (CH_3)_2CO$$

The Gibbs free energy of this reaction is +62.8 kJ mol^{-1} at 25 °C.

The most popular technique for enhancing the photocatalytic activity is the loading of electrocatalysts on semiconductor photocatalysts. For example, the photodecomposition of water on TiO_2 and $SrTiO_3$ [16–18], the photosynthesis of amino acids on TiO_2 and CdS [18–20] and the photodecomposition of saturated carboxylic acids on TiO_2 [18,21] are enhanced by noble metal loading.

In this study, we have tested the loading of several kinds of metal on ZnS microcrystal photocatalysts and found that Cd is effective in enhancing the quantum efficiency of the photoproduction of formate. On the basis of this finding, the reduction of CO_2 on solid solutions of ZnS–CdS microcrystals (which show sensitivity to visible light) has been investigated. It has been reported that ZnS–CdS co-colloids, prepared on alumina, clay and Nafion supports, show remarkable photocatalytic activity for hydrogen evolution from aqueous sulphite solutions without the loading of noble metal electrocatalysts [22]. Although an enhancement of the photocatalytic activity of CO_2 reduction is not observed by combining ZnS microcrystals with CdS, the reduction behaviour is influenced by the amount of CdS mixed with ZnS.

2. Experimental details

2.1. Preparation of ZnS and $Cd_xZn_{1-x}S$ microcrystalline colloids

The ZnS microcrystalline colloids were prepared by mixing 6×10^{-4} mol dm^{-3} (1 mol dm^{-3} = 1 M) $Zn(ClO_4)_2$ and 4×10^{-4} M Na_2S in an equal volume

* Corresponding authors.

SSDI 1010-6030(94)03936-4

in the presence of fine SiO_2 powder (Japan Aerosil, 200CF; specific surface area, 200 $m^2\ g^{-1}$) which was used as stabilizer. Details of the preparation procedures have been reported previously [14]. The resulting ZnS colloids contained excess Zn^{2+} ions (1×10^{-4} M Zn^{2+}). ZnS–CdS microcrystalline solid solution colloids given by the chemical formula $Cd_xZn_{1-x}S$ ($0\leqslant x\leqslant 1$) were prepared by a similar method to that described above. By fixing the sum of the concentrations of $Zn(ClO_4)_2$ and $Cd(ClO_4)_2$ to 6×10^{-4} M, and adding 4×10^{-4} M Na_2S to the mixed solution of $Zn(ClO_4)_2$ and $Cd(ClO_4)_2$ of equal volume, 2×10^{-4} M $Cd_xZn_{1-x}S$ microcrystalline colloids were produced in which Zn^{2+} or Cd^{2+} ions or both were in excess, with a total concentration of 1×10^{-4} M. The colloid was aged for 1 day prior to use in the CO_2 photoreduction experiments. Bulk ZnS and $Cd_xZn_{1-x}S$ colloids were also prepared using similar procedures but without SiO_2 powder as stabilizing agent. The average size of the ZnS microcrystals was 3.9 nm as reported previously [14] and that of the bulk ZnS colloids was 45 nm, as determined by a Photal DLS-70 Ar dynamic light scattering apparatus (Otsuka Electronics). The mean particle diameter of the prepared $Cd_xZn_{1-x}S$ microcrystals, evaluated by transmission electron microscopy, was about 4 nm for all cases independent of x values. On the other hand, the mean particle diameter of bulk $Cd_xZn_{1-x}S$ was 50 nm for $x=0.83$ and $x=0.75$, 60 nm for $x=0.50$ and $x=0.33$ and 80 nm for $x=0$.

2.2. Metal loading of the ZnS microcrystals

The metal loading of the ZnS particles was carried out as follows. A 3.9 cm^3 volume of the prepared ZnS colloids (0.78 μmol of ZnS) was placed in a quartz cell (1 cm×1 cm×4.5 cm) having a side branch. A 0.1 cm^3 aliquot of $Cd(ClO_4)_2$, $Pb(ClO_4)_2$, $Ni(ClO_4)_2$, $AgClO_4$ or $Cu(ClO_4)_2$ (various concentrations) was added to the ZnS colloids. Finally, 2-propanol was added as a hole scavenger to a concentration of 1 M, followed by flushing the resulting solution with Ar for 30 min to purge off the dissolved oxygen. The photodeposition of metals onto the ZnS microcrystals was then attempted by illuminating the prepared reaction solution with a 500 W high-pressure Hg arc lamp (Ushio UI-501C) through 0.1 M NaI solution to cut off UV wavelengths shorter than about 270 nm.

2.3. Photoreduction of carbon dioxide

Prior to CO_2 photoreduction experiments, 50 μl of 1.5×10^{-3} M $NaHCO_3$ was added to 4 cm^3 of the ZnS and $Cd_xZn_{1-x}S$ colloids using a microsyringe, and then CO_2 was passed through the cell for 30 min. For the metal-loaded ZnS microcrystals, the same procedures were applied just after the photodeposition of the metals. The pH of the colloids was 5.5. A 500 W high-pressure mercury arc lamp or a 500 W xenon arc lamp was used as light source, and light from the lamp was passed through a 0.1 M NaI solution for the former and a UV-39 cut-off filter (Toshiba) for the latter.

Hydrogen and carbon monoxide produced in the gas phase were determined using a gas chromatograph (Yanaco G-180), equipped with a molecular sieve 5A column (GL Sciences) and a thermal conductivity detector (TCD) (argon as carrier gas for the former and helium for the latter). Acetone produced in the liquid phase was determined using a gas chromatograph (Okura model 802) equipped with a BX-10 column (GL Sciences) and a flame ionization detector (FID). A high-pressure liquid chromatograph (Tosoh CCPD), equipped with an organic acid column (Waters) and a UV detector (Tosoh UV-8000), was used to determine the formate produced.

2.4. Determination of the quantum efficiency

The quantum efficiency was determined at 280 nm. Monochromatic light was obtained by passing light from the mercury arc lamp through a 280 nm interference filter (Oriel 280BP11). The width at half intensity was 12 nm. The number of photons absorbed by the photocatalyst was determined by subtracting the number of photons transmitted through the cell from the number of incident photons, both of which were determined by ferrioxalate actinometry.

2.5. Photochemical measurements

Absorption spectra were measured using an HP8452A diode-array spectrophotometer (Hewlett Packard). The fluorescence spectra were measured at an excitation wavelength of 280 nm using an F-3010 fluorescence spectrometer (Hitachi).

3. Results and discussion

3.1. Quantum efficiency of photoreduction of carbon dioxide using various metal-loaded zinc sulphide microcrystals

The ZnS microcrystals show absorption spectra with an onset wavelength near 315 nm, as reported previously [14]. The fluorescence spectra show a peak at around 435 nm, which is attributed to the recombination of photogenerated electrons and holes at anion vacancies [23].

Fig. 1 shows the changes in the fluorescence spectra of 2×10^{-4} M ZnS microcrystalline colloids caused by Cd loading. As described in Section 2, the ZnS microcrystalline colloids contained 1×10^{-4} M Zn^{2+} ions. On addition of 5×10^{-6} M Cd^{2+} ions, the fluorescence intensity of the colloids decreases significantly, suggesting that Cd^{2+} ions act as a quencher, but the peak fluorescence wavelength is unchanged. On the other hand, excess Zn^{2+} ions do not act as a quencher [24].

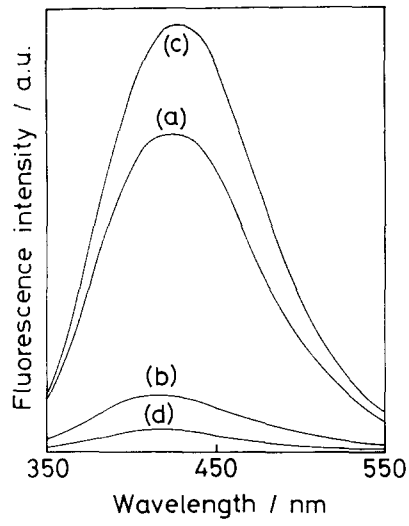

Fig. 1. Fluorescence spectra of ZnS microcrystalline colloids: (a) original ZnS microcrystalline colloids before the addition of cadmium ions; (b) after the addition of cadmium ions; (c) after subsequent illumination for 30 min with a 500 W mercury arc lamp; (d) after introduction of CO_2 for 30 min.

The inactivity of Zn^{2+} ions for fluorescence quenching may be related to their low reducibility on photoexcited ZnS microcrystals in the presence of 2-propanol. After 30 min of illumination of 4 ml of the ZnS colloids in the presence and absence of 5×10^{-6} M Cd^{2+} ions, 0.2 ml of 10 mM methyl viologen (MV^{2+}) was added to the colloids, and the amount of resulting methyl viologen cation radical ($MV^{\cdot+}$) was determined. By assuming that $MV^{\cdot+}$ is produced by reaction with the deposited metals alone, it is found that all Cd^{2+} ions present in the ZnS colloids before illumination are photodeposited, whereas only 5% of the Zn^{2+} ions are deposited by illumination for 30 min. The easy electron transfer from ZnS microcrystals to Cd^{2+} was reported by Weller et al. [23]. The results obtained here indicate that Zn^{2+} ions exhibit very weak electronic interaction with the ZnS microcrystals.

When the deposition of Cd onto ZnS microcrystals is complete, the ZnS microcrystals recover their fluorescence emission ability, as shown by spectrum (c) of Fig. 1. If CO_2 is introduced at this stage, the fluorescence intensity decreases again to give spectrum (d) of Fig. 1. The fluorescence intensity in this case is lower than that obtained for bare ZnS microcrystals in the presence of CO_2 (not shown), suggesting that photogenerated electrons are more easily scavenged by CO_2 with Cd loading. The pH of the colloids decreases from 9.0 to 5.5 on introduction of CO_2, and a pH decrease of this magnitude causes about a 75% decrease in the fluorescence intensity of Cd-loaded ZnS even if CO_2 is absent. Accordingly, the decrease in the fluorescence intensity caused by CO_2 introduction must result from both the pH change and the quenching action of CO_2.

Fig. 2 shows the time course of the production of formate and hydrogen (reduction products) and acetone (oxidation product) during the photoreduction of CO_2 in the presence of 1 M 2-propanol on the Cd-loaded ZnS microcrystals. No reduction products of CO_2 other than formate were detected, as observed on bare ZnS microcrystals [14]. The amounts of the oxidation and reduction products satisfy the chemical stoichiometry of the light-induced reactions. Since the production of these compounds occurs in proportion to the illumination time, the activity of the ZnS microcrystals remains the same for the time interval given in the figure, suggesting that the Cd deposited on the ZnS microcrystals is stable, unlike colloidal Cd [25]. The Cd-loaded ZnS microcrystals do not show any appreciable activity in the dark.

Fig. 3 shows the quantum efficiency of photoproduction of each product as a function of the molar ratio of loaded Cd to the ZnS microcrystals. For the Cd-free ZnS microcrystalline colloid, pre-illumination for 30 min was carried out before the CO_2 reduction experiments were performed. It can be seen that the quantum efficiency of photoproduction of formate is enhanced by Cd loading of the ZnS microcrystals (up to twofold larger than that obtained on bare ZnS microcrystals). The highest quantum efficiency of 42% is achieved with a Cd loading of 0.025 mol.%. If the fluorescence intensity is measured in the presence of CO_2 before the photoreduction experiments are performed, the intensity decreases with an increase in the Cd loading, as shown by the broken curve in Fig. 3, suggesting that CO_2 interacts electronically with the Cd deposited on ZnS. The quantum efficiency of formate production is saturated for loading values above 0.025 mol.%. The saturation of the photocatalytic activity with an increase in metal loading has been discussed for the photoreduction of water, using Pt-loaded TiO_2

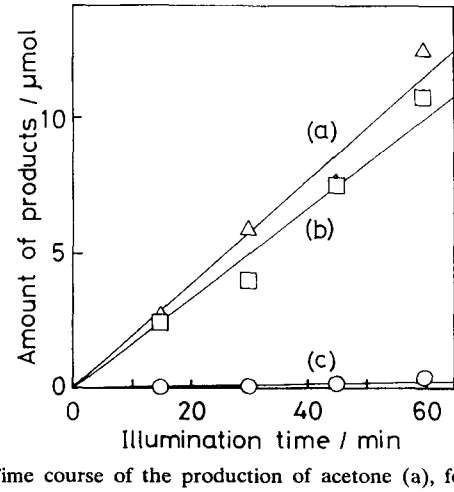

Fig. 2. Time course of the production of acetone (a), formate (b) and hydrogen (c) on Cd-loaded ZnS microcrystals. Molar ratio of Cd to ZnS microcrystals was 0.025. Other reaction conditions are given in the text.

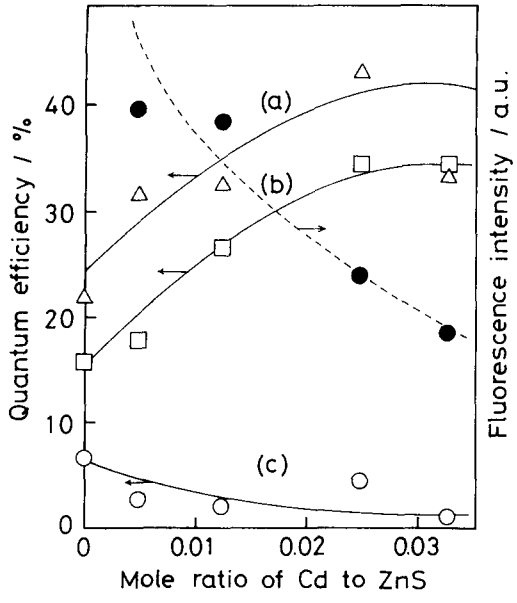

Fig. 3. Quantum efficiency of photoproduction of acetone (a), formate (b) and hydrogen (c), and the fluorescence intensity at 435 nm after the introduction of CO_2, as a function of the molar ratio of loaded cadmium on the ZnS microcrystals. Illumination time, 30 min.

and CdS powder as photocatalysts, in terms of a screening effect of the deposited metals for light absorption by the photocatalysts [26–28]. In addition, the size of deposited Cd may increase with an increase in Cd loading [29].

It may be speculated that the photoinduced reduction of CO_2 molecules on Cd-loaded ZnS microcrystals takes place with the consumption of photogenerated electrons, not only through the conduction band edge, but also through surface states associated with anion vacancies [30]. The observation that the fluorescence peaks at 435 nm for both bare and Cd-loaded ZnS microcrystals, and the absorption wavelength is 315 nm for the two kinds of photocatalyst, suggests that the anion vacancies are located at a position 1.07 V more positive than the conduction band edge. Since CO_2 quenches the fluorescence intensity as described above, the anion vacancies seem to be involved in the photoreduction of CO_2. However, it is possible that fluorescence quenching occurs even if photogenerated electrons in the conduction band move directly to the deposited metal at which the reduction of CO_2 takes place. In this regard, the involvement of the conduction band process cannot be ruled out.

Table 1 summarizes the quantum efficiencies of production of formate, hydrogen and acetone determined at 280 nm for ZnS microcrystals with various loaded metals. In the preparation of the metal-loaded photocatalysts, 5×10^{-6} M metal ions were added to the 2×10^{-4} M ZnS microcrystalline colloids in the presence of 1×10^{-4} M Zn^{2+} in all cases. As described above for the deposition of Cd, metal deposition seems to

Table 1
Quantum efficiencies of reduction and oxidation products obtained during the photoreduction of CO_2 in the presence of 2-propanol on ZnS microcrystallites having various loaded metals [a]

Photocatalyst[b]	Quantum efficiency (%)		
	Formic acid	Hydrogen	Acetone
Bulk ZnS [c]	0	15.1	24.5
Zn/ZnS	15.2	7.3	21.7
Cd/ZnS	32.5	5.0	42.0
Pb/ZnS	13.9	2.8	20.8
Ni/ZnS	10.0	8.4	17.0
Ag/ZnS	10.7	3.4	16.4
Cu/ZnS	4.9	1.7	8.3

[a] Metal loading was performed by illumination for 30 min.
[b] Experiments were carried out in the presence of 1×10^{-4} M Zn^{2+}.
[c] Bulk ZnS prepared in the absence of silica.

be completed on illumination for 30 min, except for Zn deposition where only 5% of the Zn^{2+} ions present in the solution are deposited. It may be speculated that, when the metal ions are added, replacement deposition occurs on the ZnS microcrystal surfaces even without the assistance of irradiation, because the solubility products of the sulphides of the added metal ions are smaller than that of ZnS. However, the fluorescence spectra of the ZnS microcrystalline colloids are unchanged on addition of metal ions. This suggests that the formation of the new metal sulphide by the replacement reaction does not influence significantly the fluorescence of the ZnS microcrystals.

All the loaded metals investigated in this study give formate alone. Interestingly, bulk ZnS does not show any noticeable activity for the photoreduction of CO_2. Furthermore, the loading of the metals tested in this study (except for Cd) causes a decrease in the activity for the photoreduction of CO_2. No appreciable fluorescence quenching is observed on introduction of CO_2 for Ag-, Ni- and Cu-loaded ZnS microcrystals, but fluorescence quenching is seen for Pb-loaded ZnS microcrystals, as obtained for Cd-loaded ZnS microcrystals. However, Pb-loaded ZnS shows zero activity for CO_2 reduction (Table 1). Presumably, the CO_2 adsorbed on the loaded Pb shows strong interaction with the photogenerated electrons in the ZnS microcrystals, but is not easily reduced, probably due to the high overvoltage of Pb for the reduction of CO_2 [31,32].

3.2. Photoreduction of carbon dioxide using zinc sulphide–cadmium sulphide solid solution microcrystals

The absorption spectra of $Cd_xZn_{1-x}S$ microcrystals, shown in Fig. 4, do not exhibit the characteristic absorption of CdS and ZnS, suggesting that solid solutions of CdS and ZnS are formed. With increasing content of CdS, red shifts in the absorption spectra are seen. The fluorescence spectra of $Cd_xZn_{1-x}S$ microcrystals

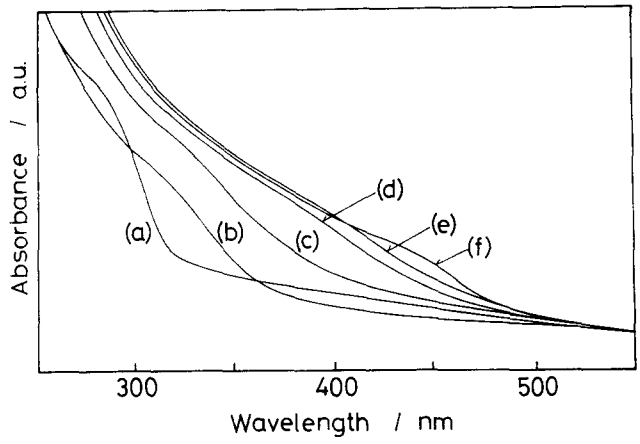

Fig. 4. Absorption spectra of $Cd_xZn_{1-x}S$ microcrystals with $x=0$ (a), $x=0.17$ (b), $x=0.25$ (c), $x=0.50$ (d), $x=0.67$ (e) and $x=1.0$ (f).

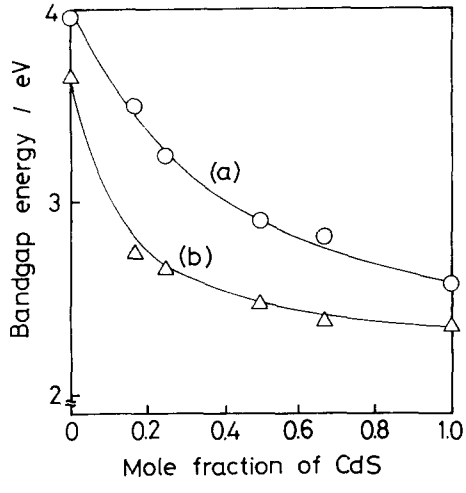

Fig. 5. Band gap energy of $Cd_xZn_{1-x}S$ microcrystals (a) and bulk $Cd_xZn_{1-x}S$ powder (b) as a function of the mole fraction of CdS.

also show one fluorescence peak irrespective of the mole fraction of CdS and this peak is red shifted with an increase in the mole fraction of CdS.

Both ZnS and CdS are semiconductors with direct band gap transitions. If it is assumed that the $Cd_xZn_{1-x}S$ microcrystals prepared in this work are semiconductors belonging to this class, the band gap energy of each $Cd_xZn_{1-x}S$ microcrystal can be evaluated by plotting $(\epsilon h\nu)^2$ vs. $h\nu$ [31] where ϵ is the molar extinction coefficient, h is the Planck constant and ν is the wavenumber. The band gap energies of various $Cd_xZn_{1-x}S$ microcrystals and bulk $Cd_xZn_{1-x}S$ powder, determined in this way, are shown in Fig. 5 as a function of the mole fraction of CdS. The band gap energy of the microcrystals is larger than that of the bulk powder for the same composition.

Fig. 6 shows the time course of the production of formate and hydrogen (reduction products) and acetone (oxidation product) when the $Cd_{0.5}Zn_{0.5}S$ microcrystals are used as photocatalyst. The reduction products are

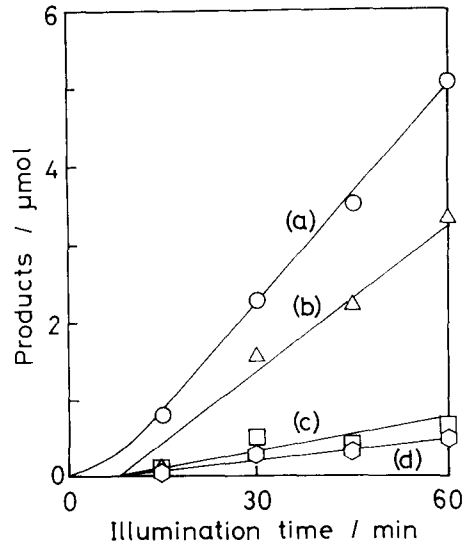

Fig. 6. Time course of the production of acetone (a), hydrogen (b), CO (c) and formate (d) on $Cd_{0.5}Zn_{0.5}S$ microcrystals. Other reaction conditions are given in the text.

produced after 8 min of illumination, while acetone is produced without a time lag. The time lag is not observed for the use of ZnS microcrystals, but for $Cd_xZn_{1-x}S$ it increases with increasing mole fraction of CdS. After the time lag, the colour of the $Cd_xZn_{1-x}S$ microcrystals changes from transparent yellow to dark brown; this returns to the original yellow colour on exposure to air, suggesting that the reduction of Cd^{2+} ions to give highly active Cd metal takes place preferentially at the start of illumination. As described in Section 2, excess Cd^{2+} ions are present in the $Cd_xZn_{1-x}S$ colloids, depending on the composition. If it is assumed that the molar ratio of excess Cd^{2+} ions to Zn^{2+} ions is equal to that of the solutions used in the preparation of $Cd_xZn_{1-x}S$ before the addition of S^{2-}, the number of moles of excess Cd^{2+} ions present in the cell increases with increasing mole fraction of CdS: 0.067, 0.10, 0.20, 0.27 and 0.40 μmol for CdS mole fractions of 0.17, 0.25, 0.50, 0.67 and 1.0 respectively. The observation that the time lag required for the formation of the reduction products (formate, CO and H_2) increases with increasing mole fraction of CdS in $Cd_xZn_{1-x}S$ suggests that the deposition of Cd^{2+} ions takes place preferentially within the time lag.

The production rates of formate, CO and hydrogen on the $Cd_xZn_{1-x}S$ microcrystals were determined from their linear dependence on the illumination time; the results are shown in Fig. 7 as a function of the mole fraction of CdS. With increasing mole fraction of CdS, the rate of formate production decreases, while hydrogen evolution increases. In the CdS mole fraction range 0.5–0.67, CO is produced as a minor reduction product of CO_2. As shown in Fig. 3, deposited Cd enhances the photocatalytic activity for CO_2 reduction to formate without producing CO. If this is taken into

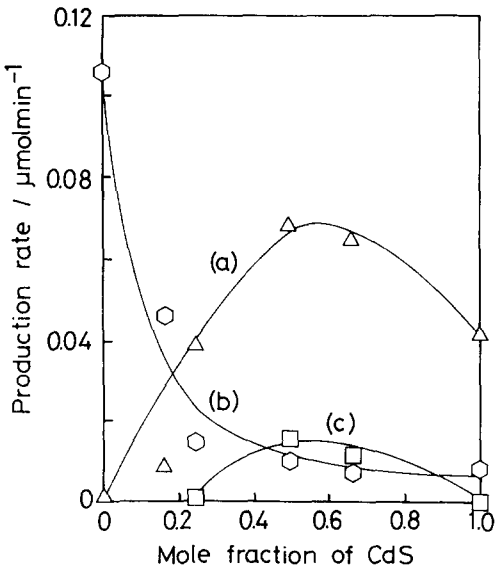

Fig. 7. Production rate of hydrogen (a), formate (b) and CO (c) on $Cd_xZn_{1-x}S$ microcrystals.

consideration, CO is not expected as a reduction product for $Cd_xZn_{1-x}S$.

The intensity of the fluorescence peak of 2×10^{-4} M $Cd_xZn_{1-x}S$ colloids (between 435 and 570 nm depending on the value of x) is quenched by the introduction of CO_2. The degree of fluorescence quenching depends on the value of x and significant quenching is observed for $Cd_xZn_{1-x}S$ microcrystals having $x=0.5$–0.67, i.e. the range in which CO production from CO_2 is seen. However, the fluorescence quenching observed is in accord with that obtained due to the variation in the pH of the colloids, suggesting that it is solely related to the adsorption of H^+ ions. It is speculated that adsorbed H^+ ions play a key role in the reduction behaviour of CO_2, although the details are unknown at present.

It can be concluded that, by preparing solid solutions of ZnS and CdS, the photocatalysts become sensitive to visible light, but the electrocatalytic activities are not enhanced.

References

[1] T. Inoue, A. Fujishima, S. Konishi and K. Honda, *Nature, 277* (1979) 637.
[2] (a) B. Aurian-Blajeni, M. Halmann and J. Manassen, *Sol. Energy, 25* (1980) 165. (b) M. Halmann, M. Ulman and B. Aurian-Blajeni, *Sol. Energy, 31* (1983) 429.
[3] (a) A. Henglein and M. Gutierrez, *Ber. Bunsenges. Phys. Chem., 87* (1983) 852. (b) A. Henglein, M. Gutierrez and Ch.-H. Fischer, *Ber. Bunsenges. Phys. Chem., 88* (1984) 170.
[4] S. Yamamura, H. Kojima, J. Iyoda and W. Kawai, *J. Electroanal. Chem., 225* (1987) 287.
[5] R.L. Cook, R.C. MacDuff and A.F. Sammells, *J. Electrochem. Soc., 135* (1988) 3069.
[6] I. Taniguchi, in J.O'M. Bockris, B.E. Conway and R.E. White (eds.), *Modern Aspects of Electrochemistry,* Vol. 20, Plenum, New York, 1989.
[7] (a) B.R. Eggins, J.T.S. Irvine, E.P. Murphy and J. Grimshaw, *J. Chem. Soc., Chem. Commun.,* (1988) 1123. (b) B.R. Eggins, P.K.J. Robertson, J.H. Stewart and E. Woods, *J. Chem. Soc., Chem. Commun.,* (1993) 349.
[8] K. Tennakone, A.H. Jayattissa and S. Punchihewa, *J. Photochem. Photobiol. A: Chem., 49* (1989) 369.
[9] (a) I. Willner and D. Mandler, *J. Am. Chem. Soc., 111* (1989) 1330. (b) Z. Goren, I. Willner, A.J. Nelson and A.J. Frank, *J. Phys. Chem., 94* (1990) 3784.
[10] S.M. Aliwi and K.F. Al-Jubori, *Sol. Energy Mater., 18* (1989) 223.
[11] P. Albers and J. Kiwi, *New J. Chem., 14* (1990) 135.
[12] K. Ogura, M. Kawano, J. Yano and Y. Sakata, *J. Photochem. Photobiol. A: Chem., 66* (1992) 91.
[13] M. Kanemoto, T. Shiragami, C. Pac and S. Yanagida, *J. Phys. Chem., 96* (1992) 3521.
[14] H. Inoue, T. Torimoto, T. Sakata, H. Mori and H. Yoneyama, *Chem. Lett.,* (1990) 1483.
[15] H. Inoue, T. Matsuyama, B.-J. Liu, T. Sakata, H. Mori and H. Yoneyama, *Chem. Lett.,* (1994) 653.
[16] M. Gratzel, in J.O'M. Bockris, B.E. Conway and R.E. White (eds.), *Modern Aspects of Electrochemistry,* Vol. 15, Plenum, New York, 1983.
[17] M.A. Fox and M.T. Dulay, *Chem. Rev., 93* (1993) 341.
[18] H. Yoneyama, *Crit. Rev. Solid State Mater. Sci., 18* (1993) 69.
[19] T. Sakata, *J. Photochem., 29* (1985) 205.
[20] H. Reiche and A.J. Bard, *J. Am. Chem. Soc., 100* (1979) 3127.
[21] (a) B. Kraeutler and A.J. Bard, *J. Am. Chem. Soc., 100* (1978) 2239. (b) B. Kraeutler, C.D. Jaeger and A.J. Bard, *J. Am. Chem. Soc., 100* (1978) 4093. (c) B. Kraeutler and A.J. Bard, *J. Am. Chem. Soc., 100* (1978) 5985.
[22] (a) N. Kakuta, K.H. Park, M.F. Finlayson, A. Ueno, A.J. Bard, A. Campion, M.A. Fox, S.E. Webber and J.M. White, *J. Phys. Chem., 89* (1985) 732. (b) A. Ueno, N. Kakuta, K.H. Park, M.F. Finlayson, A.J. Bard, A. Campion, M.A. Fox, S.E. Webber and J.M. White, *J. Phys. Chem., 89* (1985) 3828. (c) A. Ueno, N. Kakuta, K.H. Park, M.F. Finlayson, A.J. Bard, A. Campion, M.A. Fox, S.E. Webber and J.M. White, *J. Phys. Chem., 89* (1985) 5028. (d) O. Enea and A.J. Bard, *J. Phys. Chem., 90* (1986) 301. (e) J. Kobayashi, K. Kitaguchi, H. Tanaka, H. Tsuiki and A. Ueno, *J. Chem. Soc., Faraday Trans. 1, 83* (1987) 1395.
[23] H. Weller, U. Koch, M. Gutierrez and A. Henglein, *Ber. Bunsenges Phys. Chem., 88* (1984) 649.
[24] A. Henglein, *Ber. Bunsenges. Phys. Chem., 86* (1982) 301.
[25] A. Henglein and J. Lilie, *J. Phys. Chem., 85* (1981) 1246.
[26] A. Mills and G. Porter, *J. Chem. Soc., Faraday Trans. 1, 78* (1982) 3659.
[27] D.N. Furlong, D. Wells and W.H.F. Sasse, *J. Phys. Chem., 89* (1985) 1922.
[28] A.W.-H. Mau, C.B. Huang, N. Kakuta, A.J. Bard, A. Campion, M.A. Fox, J.M. White and S.E. Webber, *J. Am. Chem. Soc., 106* (1984) 6357.
[29] J.-F. Reber and M. Rusek, *J. Phys. Chem., 90* (1986) 824.
[30] M. Kanemoto, T. Shiragami, C. Pac and S. Yanagida, *J. Phys. Chem., 96* (1992) 3521.
[31] B.R. Eggins and J. McNeil, *J. Electroanal. Chem., 148* (1983) 17.
[32] Yu.B. Vassiliev, V.S. Bagotzky, N.V. Osetrova, O.A. Khazova and N.A. Mayorova, *J. Electroanal. Chem., 189* (1985) 271.